ACR No. L5B10

NATIONAL ADVISORY COMMITTEE FOR AERONAUTICS

WARTIME REPORT

ORIGINALLY ISSUED
February 1945 as
Advance Confidential Report L5B10

WIND-TUNNEL TESTS OF A BLUNT-NOSE AILERON WITH BEVELED TRAILING EDGE ON AN NACA 66(215)-216 AIRFOIL WITH SEVERAL MODIFICATIONS OF AILERON NOSE AND ADJACENT AIRFOIL CONTOUR

By J. D. Bird

Langley Memorial Aeronautical Laboratory
Langley Field, Va.

NACA

WASHINGTON

NACA ACR No. L5B10

NATIONAL ADVISORY COMMITTEE FOR AERONAUTICS

ADVANCE CONFIDENTIAL REPORT

WIND-TUNNEL TESTS OF A BLUNT-NOSE AILERON WITH BEVELED TRAILING EDGE ON AN NACA 66(215)-216 AIRFOIL WITH SEVERAL MODIFICATIONS OF AILERON NOSE AND ADJACENT AIRFOIL CONTOUR

By J. D. Bird

SUMMARY

Ailerons having a beveled trailing edge and a blunt-nose overhang of 35 percent aileron chord on an NACA 66(215)-216 airfoil have been tested in the two-dimensional-flow test section of the Langley stability tunnel. Five configurations of the model were tested with various modifications of the aileron nose and adjacent airfoil contour to determine the effect of these modifications on the lift and aileron hinge-moment characteristics.

The results indicated that making the nose of the aileron more elliptical decreased the balance of hinge moments at small aileron angles and increased the balance of hinge moments at large aileron angles. The lift coefficients, especially at large aileron angles, were increased by this modification.

Flaring the airfoil contour near the aileron nose had an effect on the hinge moments for small aileron angles similar to the effect of making the aileron nose less blunt, whereas rounding the airfoil contour had an effect similar to making the aileron nose more blunt. Flaring the airfoil contour caused a decrease in the lift resulting from aileron deflection. The effects of airfoil-contour changes were small at large aileron angles.

Comparison with other data indicated that, for small aileron angles, the increments of hinge-moment coefficient resulting from a beveled trailing edge and a blunt-nose overhang were additive.

INTRODUCTION

A beveled trailing edge or an overhang with an extremely blunt nose gives most of its balancing action at small aileron angles, whereas an overhang with a rounded blunt nose gives most of its balancing action at large aileron angles. A beveled aileron with a rounded blunt nose that fell within the contour of the airfoil at zero deflection might then be expected to have a high degree of balance over a large deflection range. The present investigation was made to determine the effect of the shape of the aileron nose and the adjacent airfoil contour on the hinge-moment and lift characteristics of such an aileron and to determine, by comparison with other data, whether the effects of the blunt-nose overhang and the beveled trailing edge on the aileron hinge-moment characteristics are additive, as has been assumed in some aileron correlations.

SYMBOLS

The coefficients and symbols used herein are defined as follows:

c_l	airfoil section lift coefficient (l/qc)
Δc_l	increment of airfoil section lift coefficient
c_h	aileron section hinge-moment coefficient $\left(h/qc_a^2\right)$
Δc_h	increment of aileron section hinge-moment coefficient
l	airfoil section lift
h	aileron section hinge moment
c	chord of airfoil
c_a	chord of aileron behind hinge axis
q	dynamic pressure $\left(\frac{1}{2}\rho V^2\right)$
V	free-stream velocity

[redacted]

ρ mass density of air

α_o angle of attack of airfoil for infinite aspect ratio

δ aileron deflection with respect to airfoil

$a_\delta = \frac{\partial a_o}{\partial \delta}$ at $c_l = 0.1$

$c_{h_\alpha} = \frac{\partial c_h}{\partial a_o}$ at $\delta = 0^\circ$

$c_{h_\delta} = \frac{\partial c_h}{\partial \delta}$ at $a_o = 0^\circ$

$c_{l_\alpha} = \frac{\partial c_l}{\partial a_o}$ at $\delta = 0^\circ$

$c_{l_\delta} = \frac{\partial c_l}{\partial \delta}$ at $a_o = 0^\circ$

w airfoil-contour configuration in region adjacent to aileron nose

n aileron-nose configuration

Subscripts 1 to 4 to w and n indicate configurations as given in figure 1 and table I. Configuration designations are used as subscripts to identify corresponding lift and hinge-moment coefficients.

APPARATUS AND MODEL

Tests were made in the two-dimensional-flow test section of the Langley stability tunnel. This section is rectangular, 6 feet high, and 2.5 feet wide.

The model tested had an NACA 66(215)-216 airfoil section of 2-foot chord and completely spanned the width of the test section. Table II gives the airfoil ordinates.

[redacted]

The aileron had a chord of 0.20c, a $0.35c_a$ blunt-nose balance, and a 26° beveled trailing edge. The five aileron and airfoil configurations are described in table I and figure 1.

TEST CONDITIONS

Hinge moments were measured with a spring hinge-moment balance, and lift was measured by an integrating manometer connected to orifices in the floor and ceiling of the tunnel. The hinge moments and lifts were measured for a range of aileron angles from 0° to ±25° and for an angle-of-attack range from 0° to ±10°. The tests were made at a dynamic pressure of 230 pounds per square foot, which corresponds to a Mach number of 0.42 and to a test Reynolds number of 6×10^6 based on standard sea-level atmospheric conditions. All five configurations were tested with the gap at the aileron nose sealed and unsealed. Angles of attack were set within ±0.1° and aileron angles, within ±0.3°. Hinge-moment coefficients are believed to be accurate to ±0.003 and lift coefficients, to ±0.01. The data were corrected for jet-boundary effects. The corrected values were computed as follows:

$$\alpha_o = 1.023\alpha_{o_T}$$

$$c_l = 0.963c_{l_T}$$

$$c_h = c_{h_T} + 0.0043c_{l_T}$$

where α_{o_T}, c_{l_T}, and c_{h_T} are the uncorrected angle of attack in degrees, lift coefficient, and hinge-moment coefficient.

RESULTS AND DISCUSSION

Presentation of Data

The section lift and aileron section hinge-moment characteristics are given in figures 2 to 6 for the

[redacted]

various airfoil-contour and aileron-nose configurations tested. The increments of lift and hinge-moment coefficients resulting from the modifications are plotted in figures 7 to 12. Some of the data and important parameters from references 1 and 2 are compared with results of the present tests in figures 13 to 18 and table III.

Effect of Modifications on Lift and Hinge-Moment Characteristics

Sealed ailerons.- Figure 7(a) shows, for gap sealed, the increments Δc_h that result from rounding the airfoil contour adjacent to the aileron nose. The curves indicate that, in general, the balance is increased for aileron angles up to approximately $\pm 10^\circ$ but that, for angles greater than $\pm 10^\circ$, the change in balance is decreased to a small value at the largest positive or negative angles. These results indicate that this modification gives results similar to those obtained when an aileron nose is made more blunt.

The increments Δc_h caused by flaring the airfoil contour in the area adjacent to the aileron nose are shown in figure 8(a) for gap sealed. The flare decreases the degree of balance for aileron angles up to approximately $\pm 14^\circ$, beyond which the balance is increased almost to the value for configuration $w_1 n_1$. This loss in balance at small deflections is caused by the shielding effect of the flare, which gives results similar to those obtained when an aileron nose is made less blunt.

The curves of figure 9(a) show, for gap sealed, the increments Δc_h caused by making the aileron nose more nearly elliptical. These curves indicate that this modification decreases the degree of balance for aileron angles up to approximately $\pm 10^\circ$ and increases the balance for the rest of the aileron-angle range.

Figure 10(a) shows, for the gap sealed, the increments Δc_l caused by increased rounding of the airfoil contour in the area adjacent to the aileron nose. The curves, though quite irregular, generally indicate an increase of about 4 percent in c_{l_δ} for small aileron angles.

[redacted]

The increments Δc_l that result from flaring the airfoil contour in the area adjacent to the aileron nose are given in figure 11(a) for gap sealed. These curves indicate a loss of approximately 10 percent in c_{l_δ} for aileron angles up to approximately $\pm 12^\circ$. For large aileron angles, the lift coefficient increases to approximately the value obtained for the unmodified airfoil (configuration w_1n_1).

Figure 12(a) shows, for gap sealed, the increments Δc_l that result from making the aileron nose more nearly elliptical. These curves indicate an appreciable increase in lift coefficient for large aileron angles. This large increase occurs at positive and negative aileron angles from 12° to 24°, because the aileron with the more elliptical nose stalls at larger aileron angles than the aileron with the rounded blunt nose. The sealed aileron gave an increase of about 4 percent in c_{l_δ} for aileron angles up to $\pm 12^\circ$.

Unsealed ailerons.- The principal effect of removing the seal (figs. 7(b), 8(b), 9(b), 10(b), and 11(b)) is to accentuate the effects of contour modification on the values of c_h and c_l shown for the sealed gaps. The results given in figure 12(b), however, are an exception to this statement.

General remarks.- It is believed that more nearly linear hinge-moment characteristics could be obtained if the aileron overhang were slightly longer and more elliptical than the overhangs tested. Such a configuration would allow the overhang to produce more balance at large deflections for which the degree of balance due to the beveled trailing edge is reduced. With the overhangs tested, the hinge-moment characteristics showed a definite tendency toward increased linearity as the overhang was made more elliptical; however, the overhang was not long enough nor elliptical enough to obtain the linear hinge-moment characteristics expected.

Increments Δc_h Caused by Beveled Trailing Edge and by Overhang

For a number of correlations of aileron hinge-moment characteristics, the assumption has been made that the

increments of hinge-moment coefficient caused by different aileron balances, such as overhangs and bevels, are additive when these aileron balances are used with each other. The validity of this assumption is investigated in figures 13 and 14 for the blunt-nose aileron with a beveled trailing edge.

Figure 13 compares the variation of c_h with δ at $\alpha_o = 0^\circ$ for the cusped plain aileron (unpublished data), the plain aileron with a 26° beveled trailing edge (estimated from unpublished data), the cusped aileron with a $0.35c_a$ blunt-nose overhang (reference 1), and the aileron with a 26° beveled trailing edge and a $0.35c_a$ blunt-nose overhang (fig. 2(a)). All these data are for sealed 0.20c ailerons on the same airfoil and therefore should be comparable. The data for the plain aileron with the 26° beveled trailing edge were estimated from unpublished data for a cusped plain aileron and for a straight-side plain aileron on the assumption that the change in c_h is a linear function of the trailing-edge angle.

Figure 14(a), which was obtained from figure 13, shows that the increments Δc_h caused by the bevel on plain ailerons and on ailerons with blunt-nose overhang are in good agreement for aileron angles from approximately -8° to 4°; figure 14(b) shows that the increments Δc_h caused by the blunt-nose overhang on cusped and on beveled ailerons also are in good agreement for this range of aileron angles. The curves show less good agreement for aileron angles outside the range from -8° to 4°. This lack of agreement at large aileron angles may be caused by the effect of the blunt nose on the air flow over the bevel. The curves of figure 14 also indicate that the 26° beveled trailing edge produced much more balance than the $0.35c_a$ blunt-nose overhang.

Comparison with Other Ailerons

The hinge-moment and lift characteristics for the aileron having a 26° beveled trailing edge and a $0.35c_a$ blunt-nose overhang (configuration w_1n_1) are compared in figures 15 to 18 with the characteristics for cusped ailerons of references 1 and 2 having a $0.35c_a$ blunt-nose overhang and a $0.60c_a$ internal balance,

respectively. All three ailerons had sealed gaps, had the same chord, and were on the same airfoil.

Figure 15 indicates that the internally balanced aileron has a greater linear range of c_h against δ and a slope c_{h_δ} nearer zero than either of the other two ailerons. The cusped aileron with blunt-nose overhang produced the least balance. A slight positive value of c_{h_δ} is shown at $\alpha_o = 0^\circ$ for the beveled aileron with the blunt-nose overhang. This overbalance is counteracted to some extent by the positive c_{h_α} shown for this aileron in figure 16.

The cusped aileron with internal balance and the cusped aileron with blunt-nose overhang have negative values of c_{h_α} (fig. 16). The negative value of c_{h_α} would generally cause the internally balanced aileron to be overbalanced for a large range of the aileron deflection (where $c_{h_\delta} = 0$). Slightly less balance-plate chord should make it possible for this aileron to operate without being overbalanced. Overbalance would probably not occur with the blunt-nose aileron since it has a negative value of c_{h_δ}.

Figure 17 and table III indicate that, of the three ailerons considered, the cusped aileron with the blunt-nose overhang has the largest value of c_{l_δ}. Both the cusped and beveled ailerons having the blunt-nose overhang stall at a lower deflection than the internally balanced aileron. The internally balanced aileron, which has no projecting nose, therefore produces higher positive and negative lifts at large deflections than the other two ailerons. As might be expected, the aileron with the beveled trailing edge produces a smaller lift than the cusped ailerons.

The values of c_{l_α} as given in table III and the curves of c_l plotted against α_o for $\delta = 0^\circ$ (fig. 18) indicate that the cusped aileron with blunt-nose overhang has the largest value of c_{l_α} and that the aileron with the beveled trailing edge and blunt-nose overhang has the lowest value.

[redacted]

CONCLUSIONS

Ailerons having a 0.35-aileron-chord blunt-nose overhang and a 26° beveled trailing edge have been tested in two-dimensional flow on an NACA 66(215)-216 airfoil with several modifications of the aileron nose and adjacent airfoil contour. The results of these tests and comparison with results of previous tests of cusped internally balanced and blunt-nose ailerons indicated the following conclusions:

1. Making the aileron nose more nearly elliptical decreased the balance of hinge moments at small aileron angles and increased the balance of hinge moments at large aileron angles. The lift coefficients at large angles were higher than those obtained with the more blunt nose.

2. Rounding the airfoil contour adjacent to the aileron nose generally increased the balance of hinge moments and, for small aileron angles, slightly increased the value of the slope of the curve of lift coefficient against aileron angle c_{l_δ}. The increase in balance was most pronounced for a range of aileron angle of ±10°. This modification gave results similar to those that would be obtained when an aileron nose is made more blunt.

3. Flaring the airfoil contour in the region adjacent to the aileron nose decreased the balance of hinge moments for aileron angles up to approximately ±14°. The value of c_{l_δ} over a large part of the aileron-angle range was decreased. These results were similar to those that would be obtained when an aileron nose is made less blunt.

4. The effects of the airfoil-contour changes were small at large aileron angles.

5. Unsealing the gap at the aileron nose generally caused the effects resulting from the various modifications of the aileron nose and adjacent airfoil contour to be more pronounced.

6. The aileron with 0.60-aileron-chord internal balance and cusped trailing edge afforded a greater degree of balance of hinge moments and higher lift at large deflections than the cusped aileron with the 0.35-aileron-chord blunt-nose

[redacted]

overhang or the aileron with 26° beveled trailing edge and 0.35-aileron-chord blunt-nose overhang.

7. Comparison with other data indicated that, for small aileron angles, the increments of hinge-moment coefficient resulting from a beveled trailing edge and a blunt-nose overhang were additive.

Langley Memorial Aeronautical Laboratory
National Advisory Committee for Aeronautics
Langley Field, Va.

REFERENCES

1. Letko, W., Denaci, H. G., and Freed, C.: Wind-Tunnel Tests of Ailerons at Various Speeds. I - Ailerons of 0.20 Airfoil Chord and True Contour with 0.35 Aileron-Chord Extreme Blunt Nose Balance on the NACA 66,2-216 Airfoil. NACA ACR No. 3F11, 1943.

2. Denaci, H. G., and Bird, J. D.: Wind-Tunnel Tests of Ailerons at Various Speeds. II - Ailerons of 0.20 Airfoil Chord and True Contour with 0.60 Aileron-Chord Sealed Internal Balance on the NACA 66,2-216 Airfoil. NACA ACR No. 3F18, 1943.

[redacted]

TABLE I.- AIRFOIL-CONTOUR AND AILERON-NOSE CONFIGURATIONS

Configuration	Airfoil contour adjacent to aileron nose	Aileron nose shape
w_1n_1	True	Rounded blunt
w_2n_1	Flared	Do.
w_3n_1	Rounded	Do.
w_3n_2	----------do----------	More nearly elliptical than n_1
w_4n_2	More rounded than w_3	Do.

NATIONAL ADVISORY
COMMITTEE FOR AERONAUTICS

TABLE II.- ORDINATES FOR NACA 66(215)-216 AIRFOIL[1]

[Basic airfoil contour; stations and ordinates in percent airfoil chord]

Upper surface		Lower surface	
Station	Ordinate	Station	Ordinate
0	0	0	0
.401	1.230	.599	-1.130
.640	1.484	.860	-1.344
1.128	1.858	1.372	-1.644
2.362	2.560	2.638	-2.188
4.846	3.604	5.154	-2.972
7.340	4.428	7.660	-3.580
9.838	5.140	10.162	-4.106
14.845	6.276	15.155	-4.930
19.860	7.156	20.140	-5.564
24.879	7.844	25.121	-6.054
29.900	8.366	30.100	-6.422
34.924	8.736	35.076	-6.676
39.949	8.980	40.051	-6.838
44.974	9.092	45.026	-6.902
50.000	9.060	50.000	-6.854
55.025	8.875	54.975	-6.685
60.048	8.496	59.952	-6.354
65.067	7.862	64.933	-5.802
70.081	6.941	69.919	-4.997
75.087	5.860	74.913	-4.070
80.085	4.644	79.915	-3.052
85.075	3.395	84.925	-2.049
90.055	2.103	89.945	-1.069
95.028	.913	94.972	-.281
100.000	0	100.000	0
L. E. radius: 1.575. Slope of radius through L. E.: 0.084			

[1]This airfoil is the same as NACA 66,2-216 airfoil, for which the designation has been changed since references 1 and 2 were published.

NATIONAL ADVISORY
COMMITTEE FOR AERONAUTICS

[redacted]

TABLE III.- LIFT AND HINGE-MOMENT PARAMETERS MEASURED AT $\alpha_o = 0^\circ$ AND $\delta = 0^\circ$ EXCEPT FOR α_δ MEASURED AT $c_l = 0.1$ BETWEEN $\delta = \pm 10^\circ$

[Sealed ailerons; Mach number ≈ 0.4]

Aileron	Airfoil contour (1)	Aileron nose (1)	c_{l_α}	c_{l_δ}	α_δ	c_{h_δ}
Blunt nose with beveled T. E.	w_1	n_1	0.095	0.039	-0.37	0.003
Blunt nose[2] (reference 1)	w_1	n_1	.118	.058	-.43	-.004
Internally balanced[2] (reference 2); vent gap, 0.005c	-------	-------	.113	.050	-.42	0

[1]As designated in fig. 1 and table I.
[2]True airfoil contour.

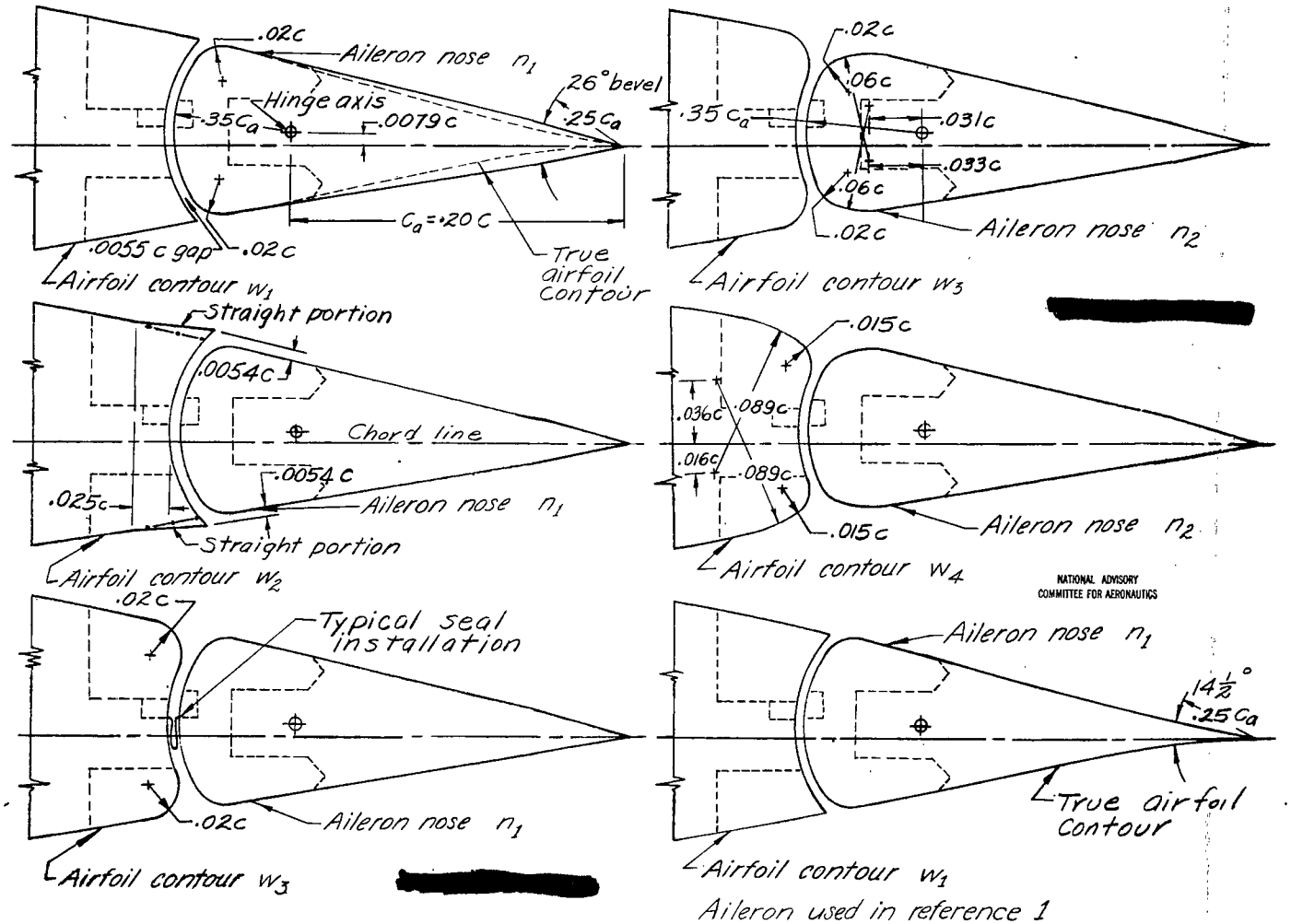

Figure 1. - Sketches of aileron and airfoil contour configurations. c = 24 inches. Bevel is symmetrical about line through hinge axis to trailing edge; dashed lines indicate removable sections.

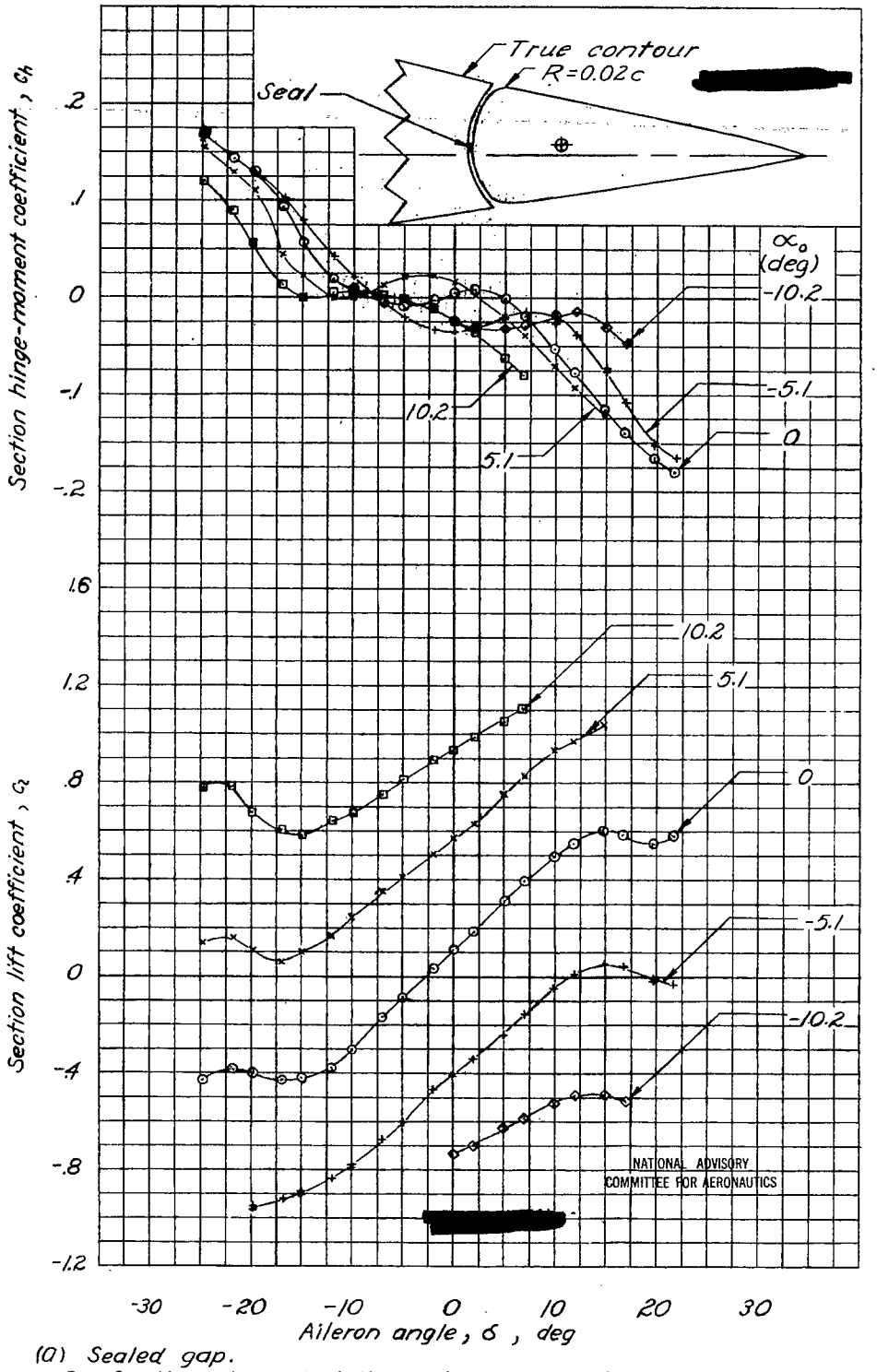

(a) Sealed gap.

Figure 2.- Section characteristics of blunt-nose aileron with beveled trailing edge. Airfoil contour w_1; aileron nose n_1.

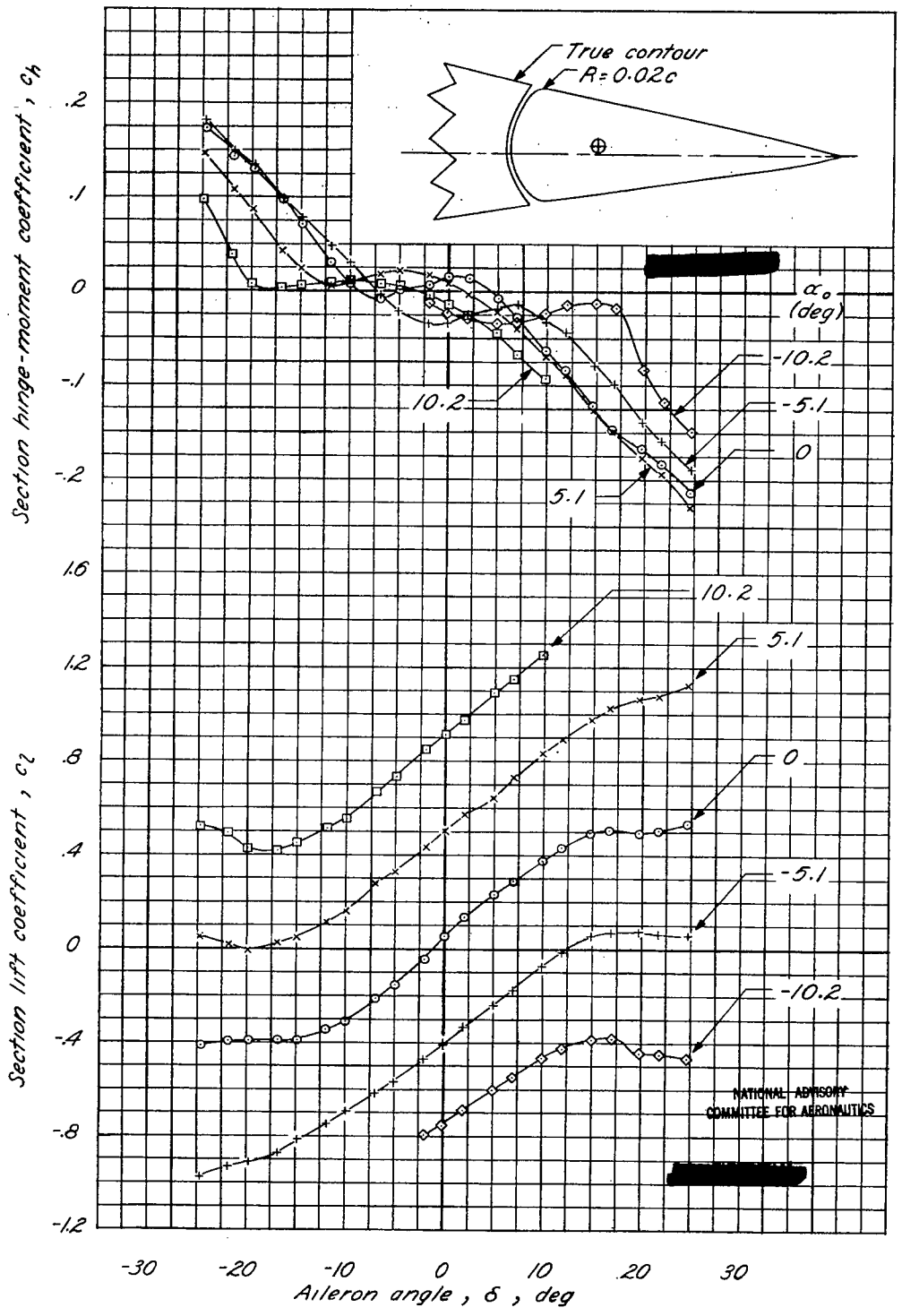

(b) Unsealed gap.

Figure 2. — Concluded.

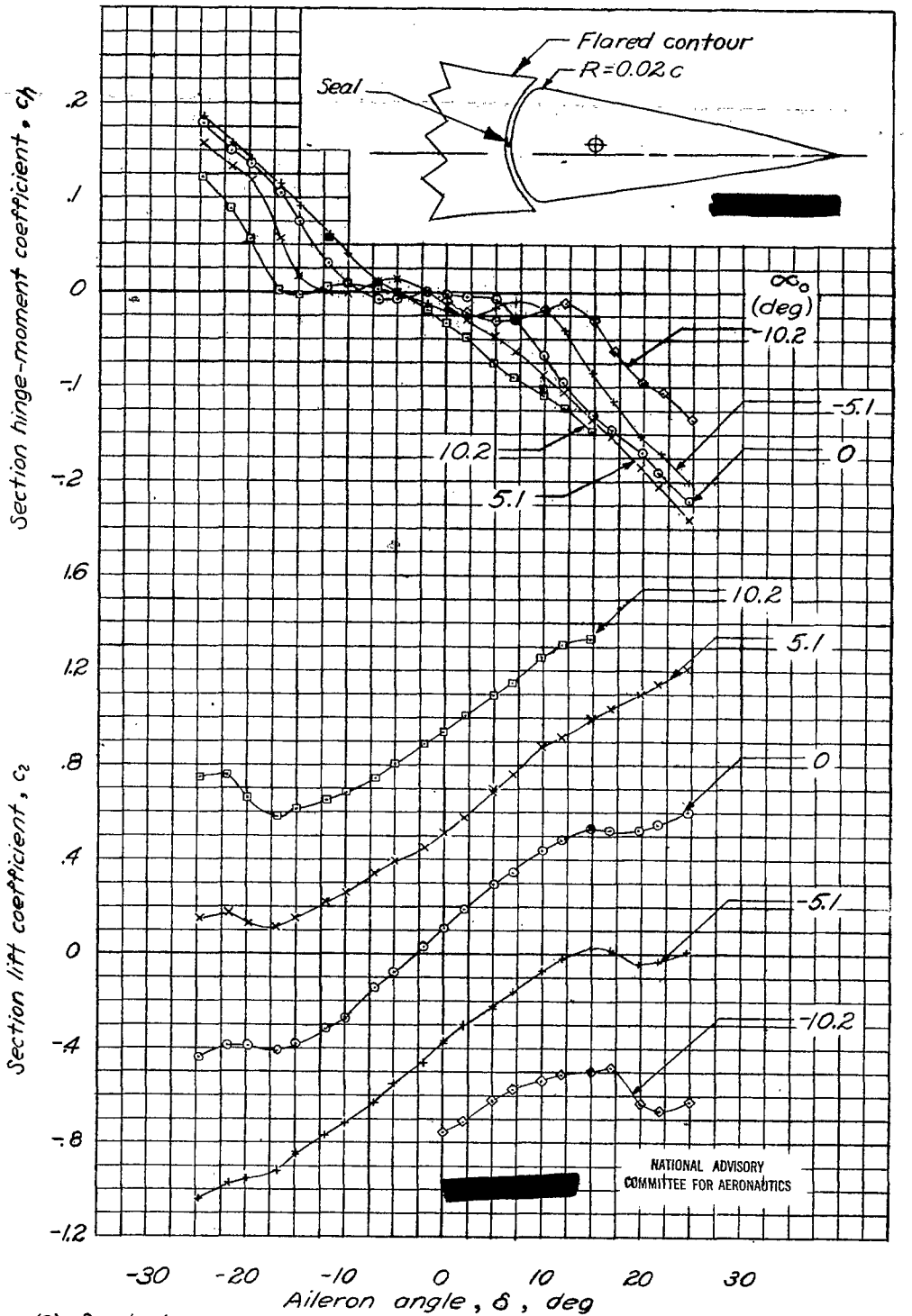

(a) Sealed gap.

Figure 3.- Section characteristics of blunt-nose aileron with beveled trailing edge. Airfoil contour w_2; aileron nose n_1.

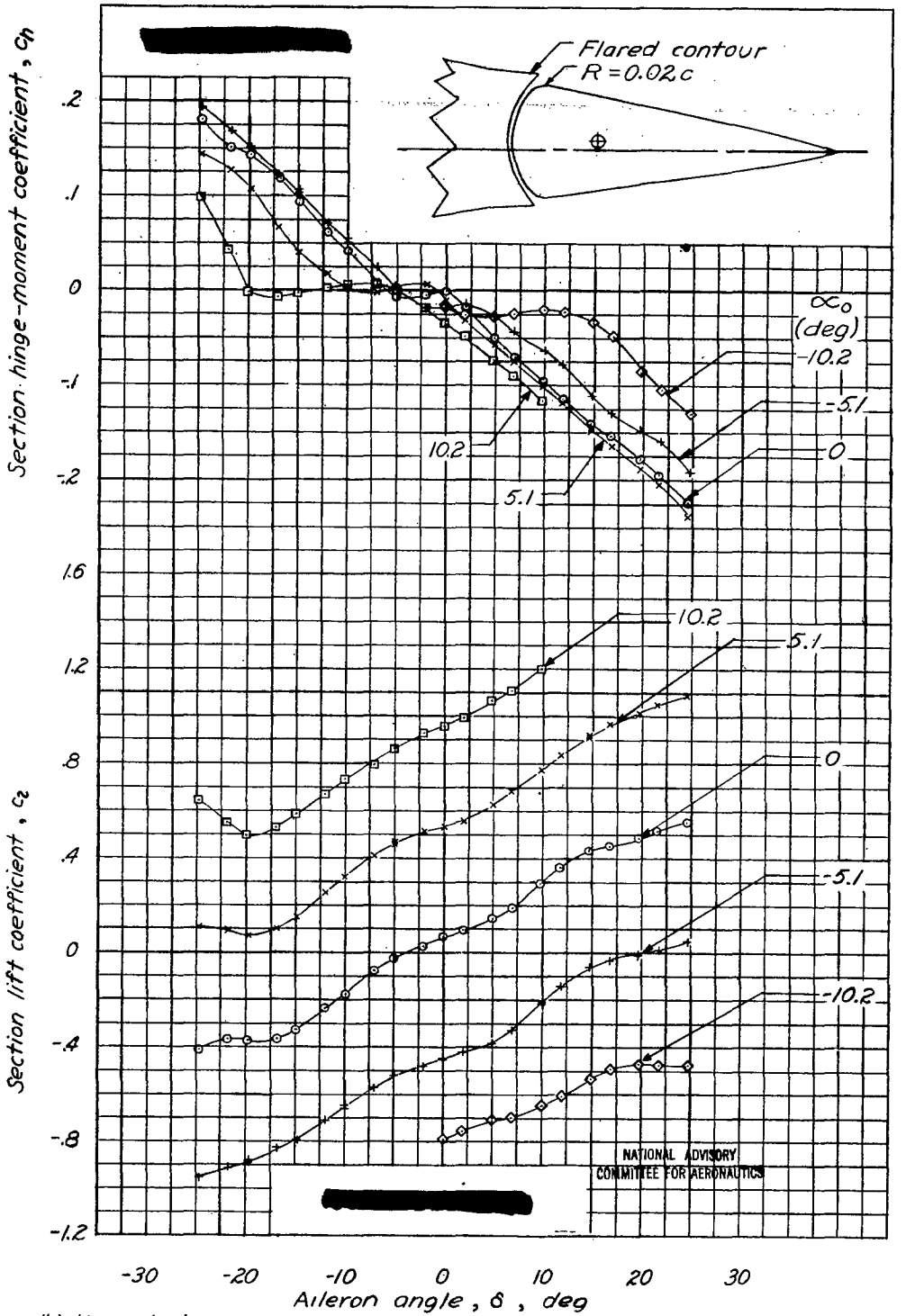

(b) Unsealed gap.

Figure 3.– Concluded.

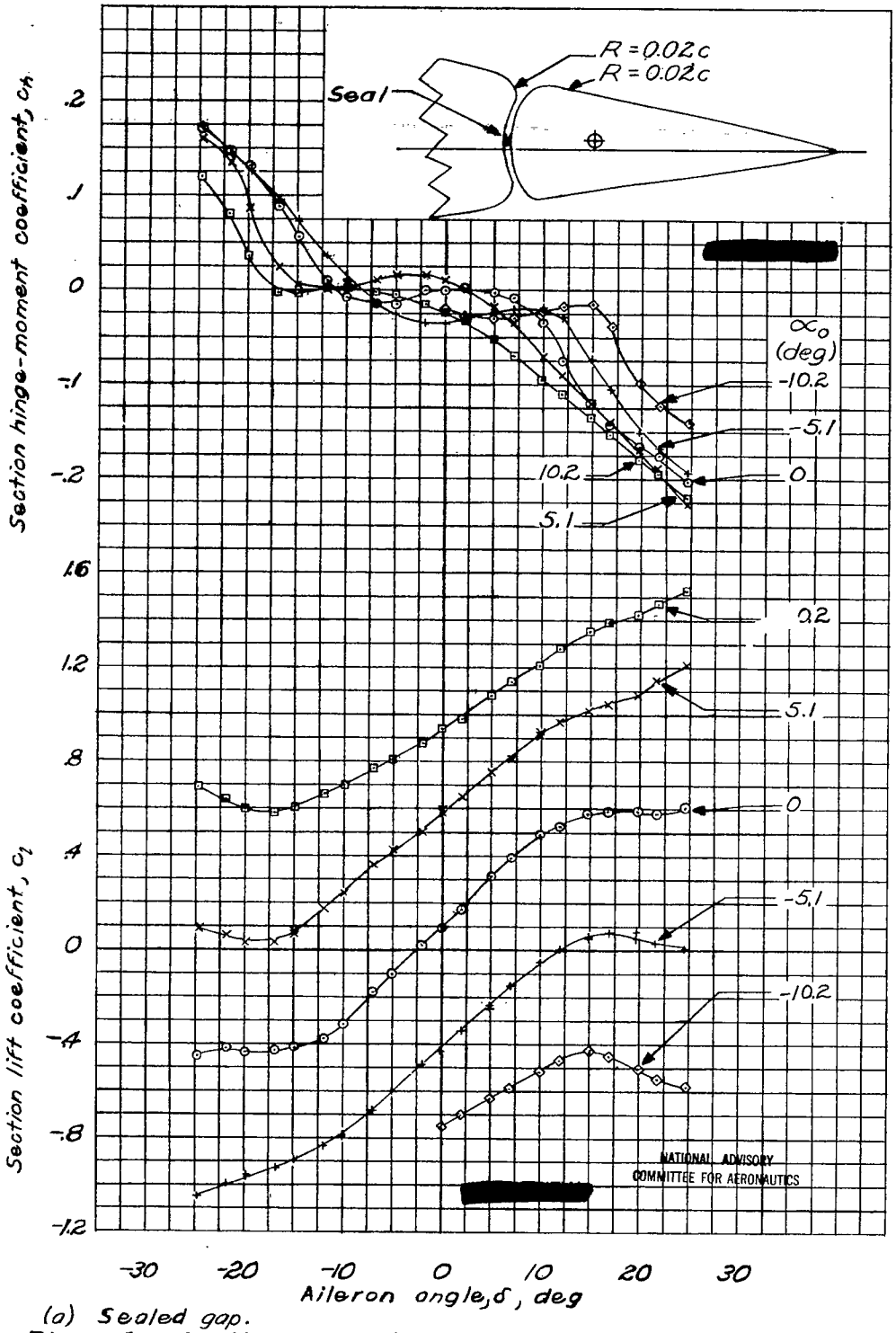

(a) Sealed gap.

Figure 4.- Section characteristics of blunt-nose aileron with beveled trailing edge. Airfoil contour W_3; aileron nose n_1.

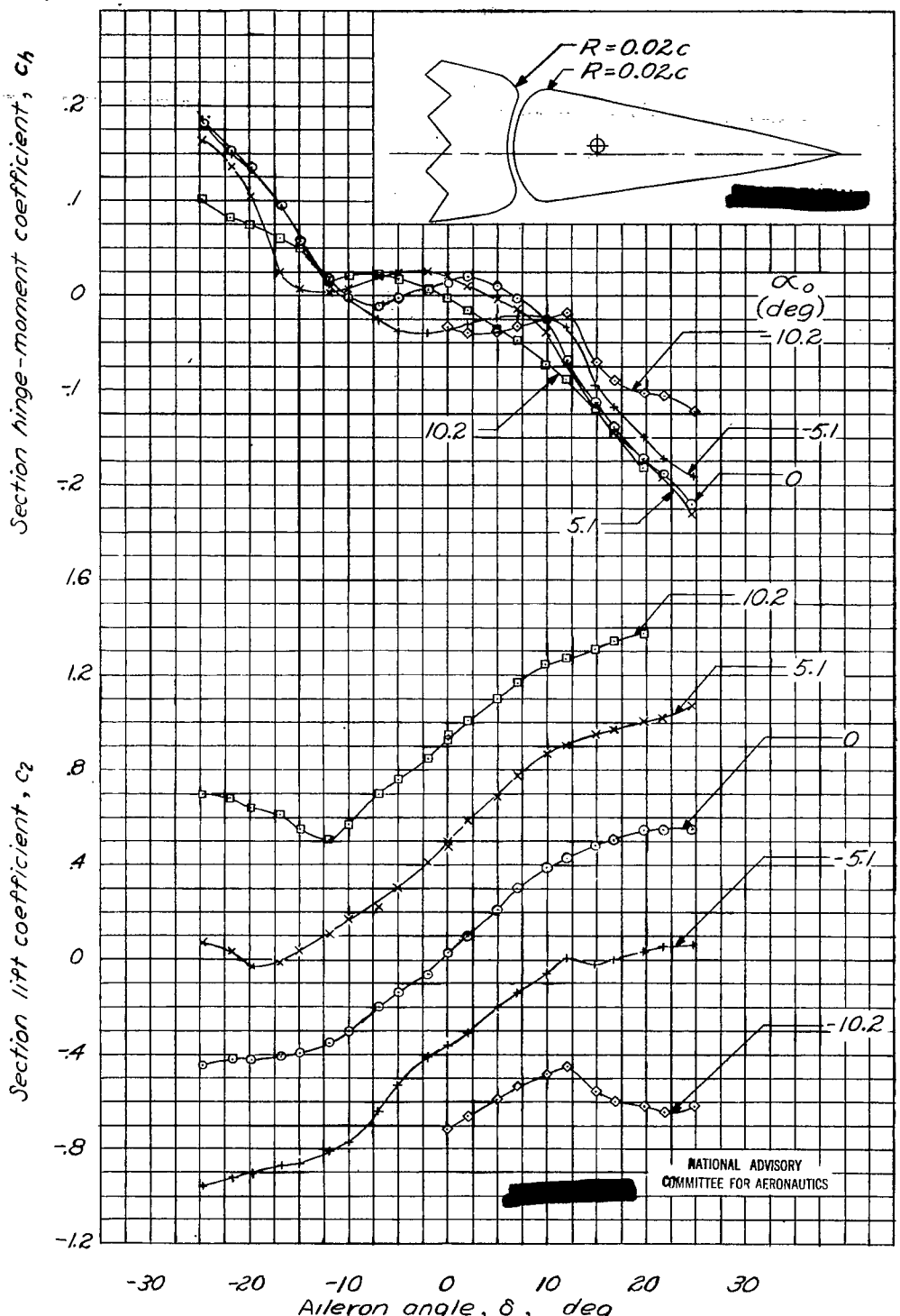

(b) Unsealed gap.

Figure 4.- Concluded.

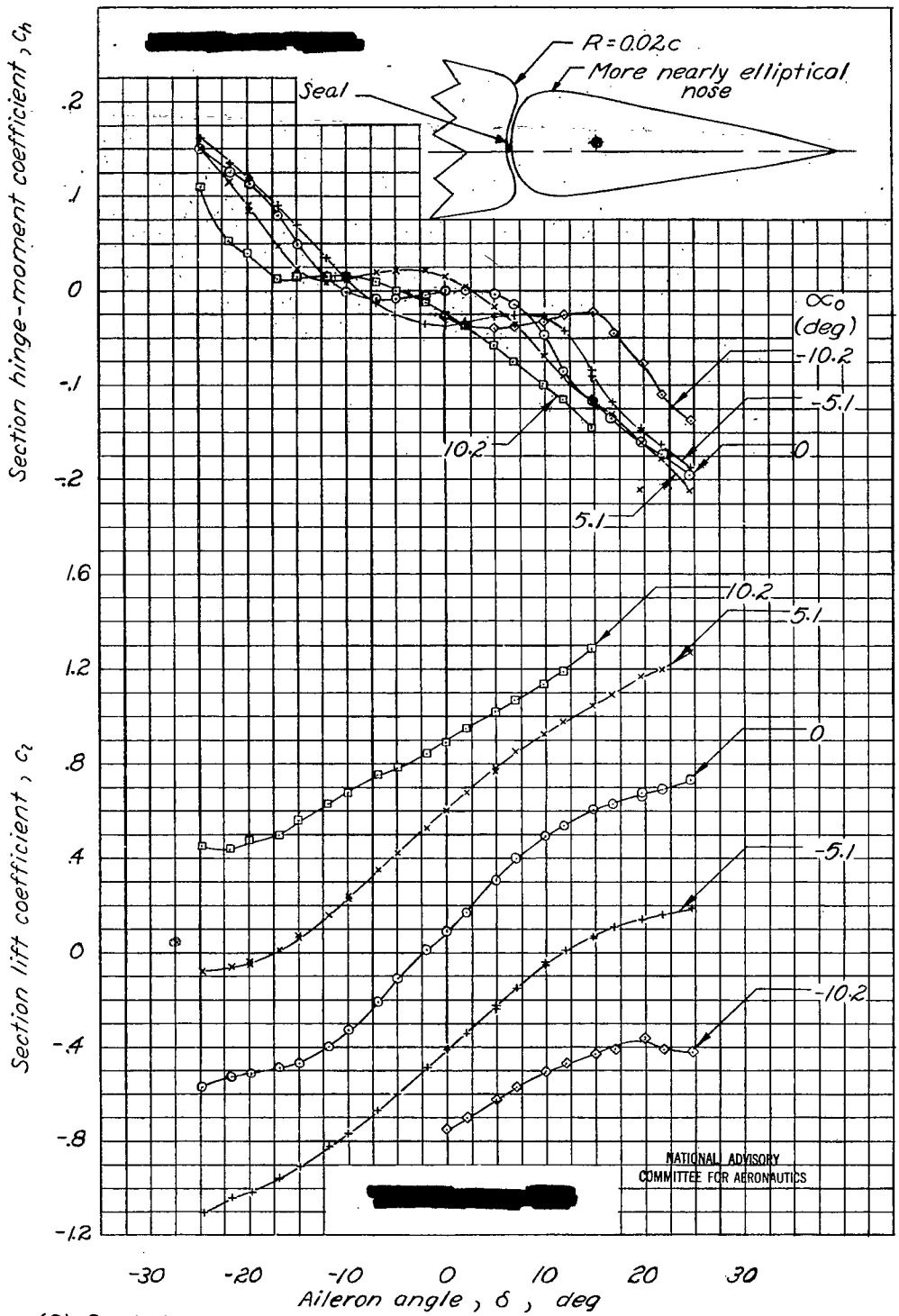

(a) Sealed gap.

Figure 5.— Section characteristics of blunt-nose aileron with beveled trailing edge. Airfoil contour w_3; aileron nose n_2.

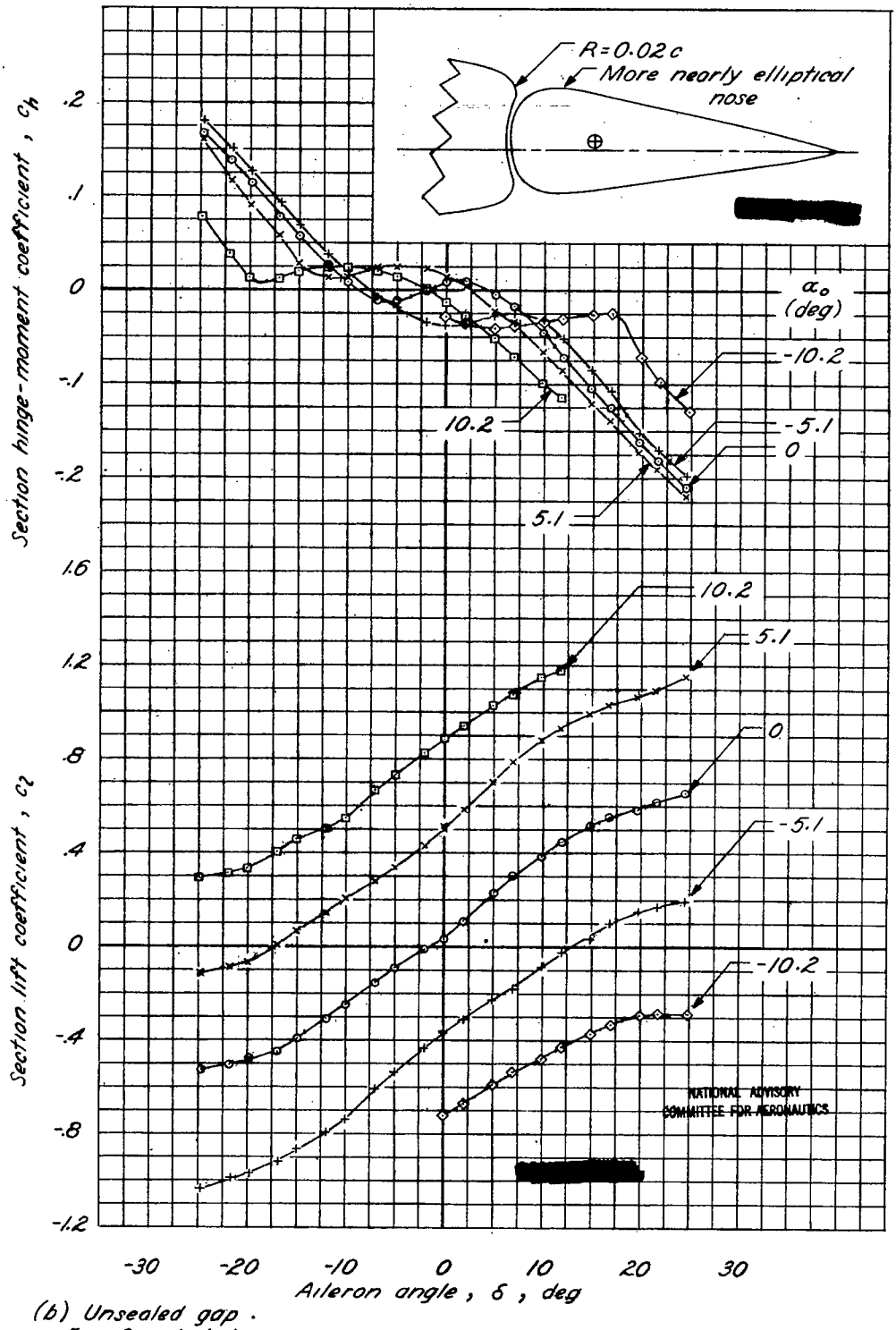

(b) Unsealed gap.

Figure 5.- Concluded.

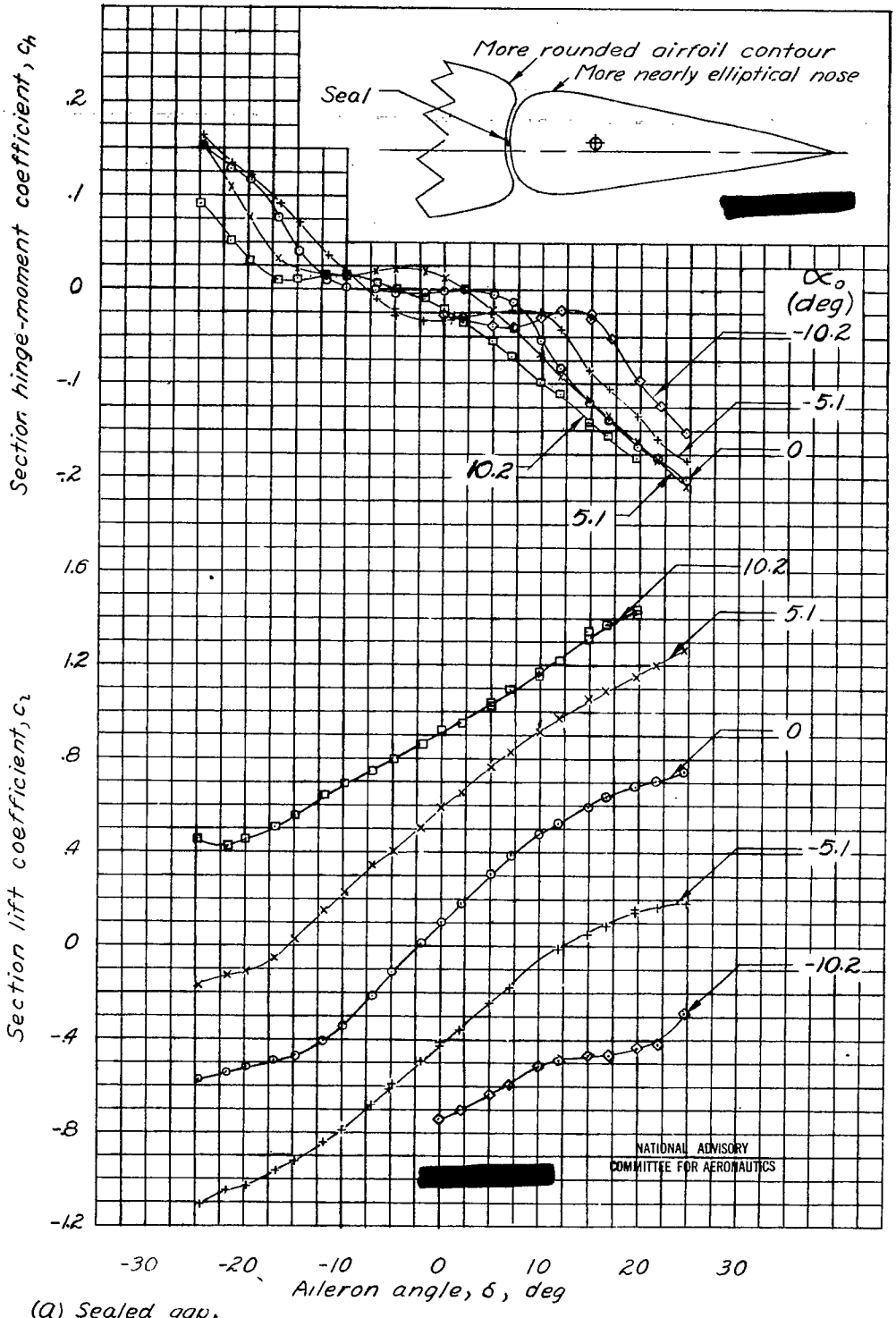

(a) Sealed gap.

Figure 6.- Section characteristics of blunt-nose aileron with beveled trailing edge. Airfoil contour, w_4; aileron nose, n_2.

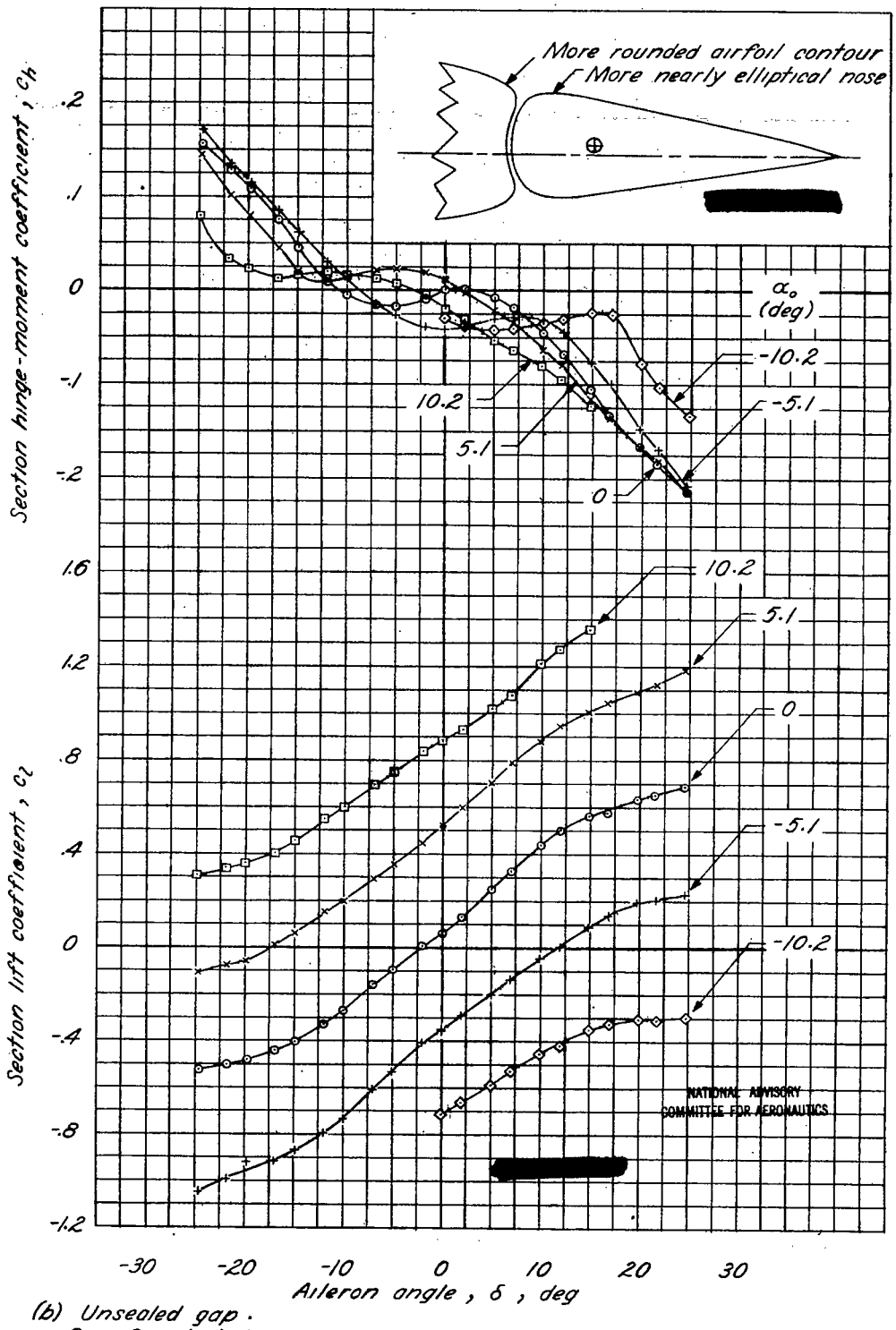

(b) Unsealed gap.

Figure 6.- Concluded.

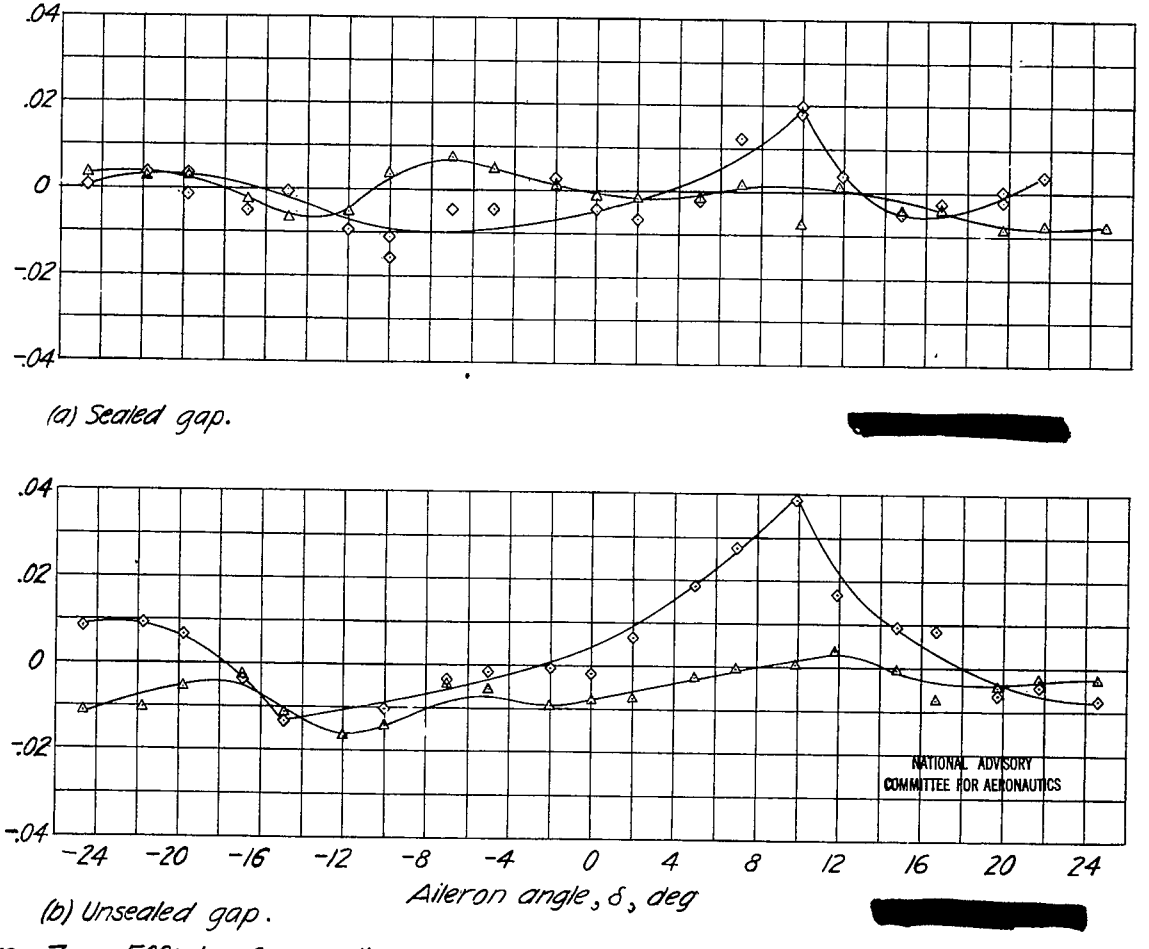

Figure 7.—Effect of rounding airfoil contour adjacent to aileron nose on section hinge-moment characteristics of aileron. $\alpha_o = 0°$.

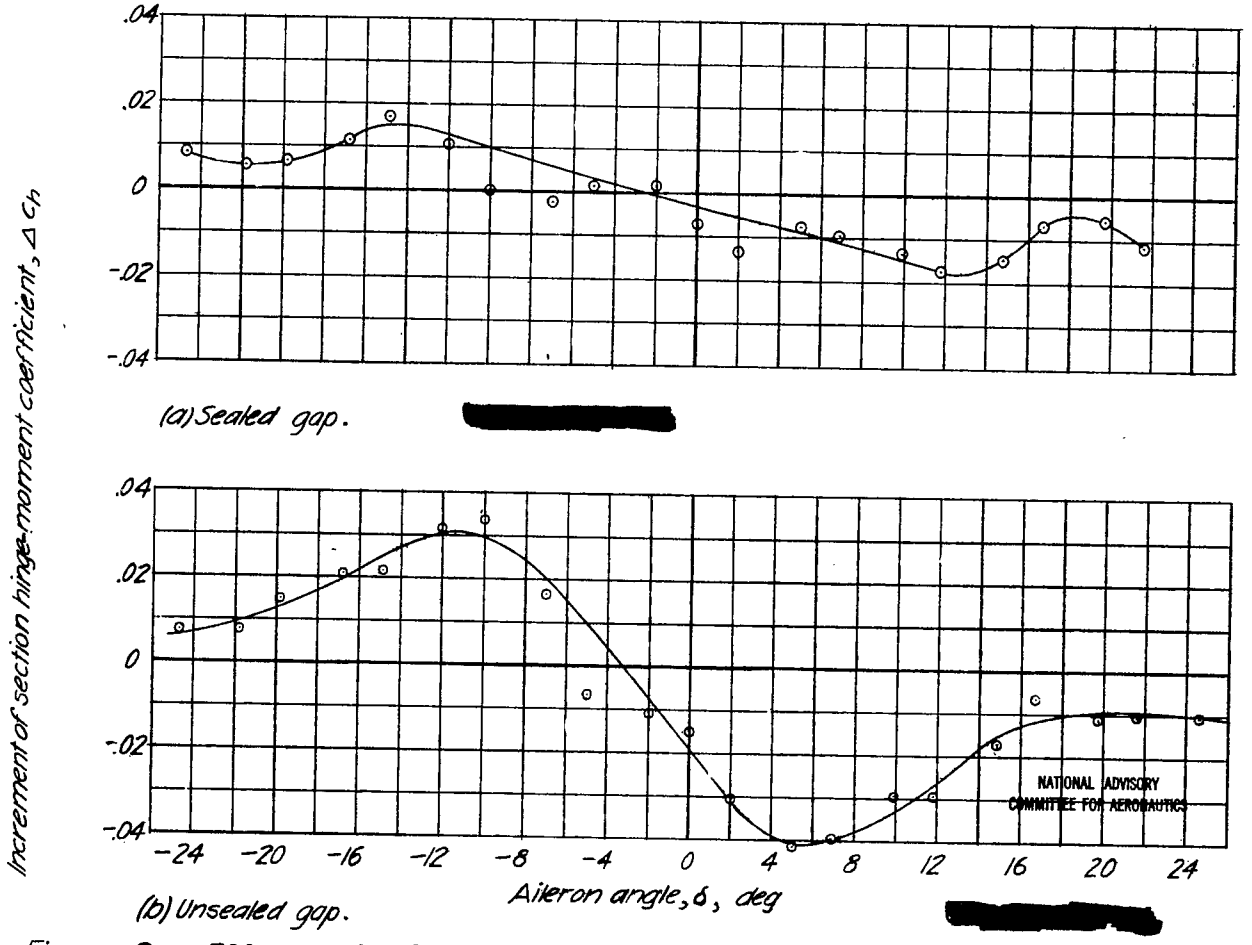

Figure 8.— Effect of flaring airfoil contour adjacent to aileron nose on section hinge-moment characteristics of aileron. $\alpha_o = 0°$.

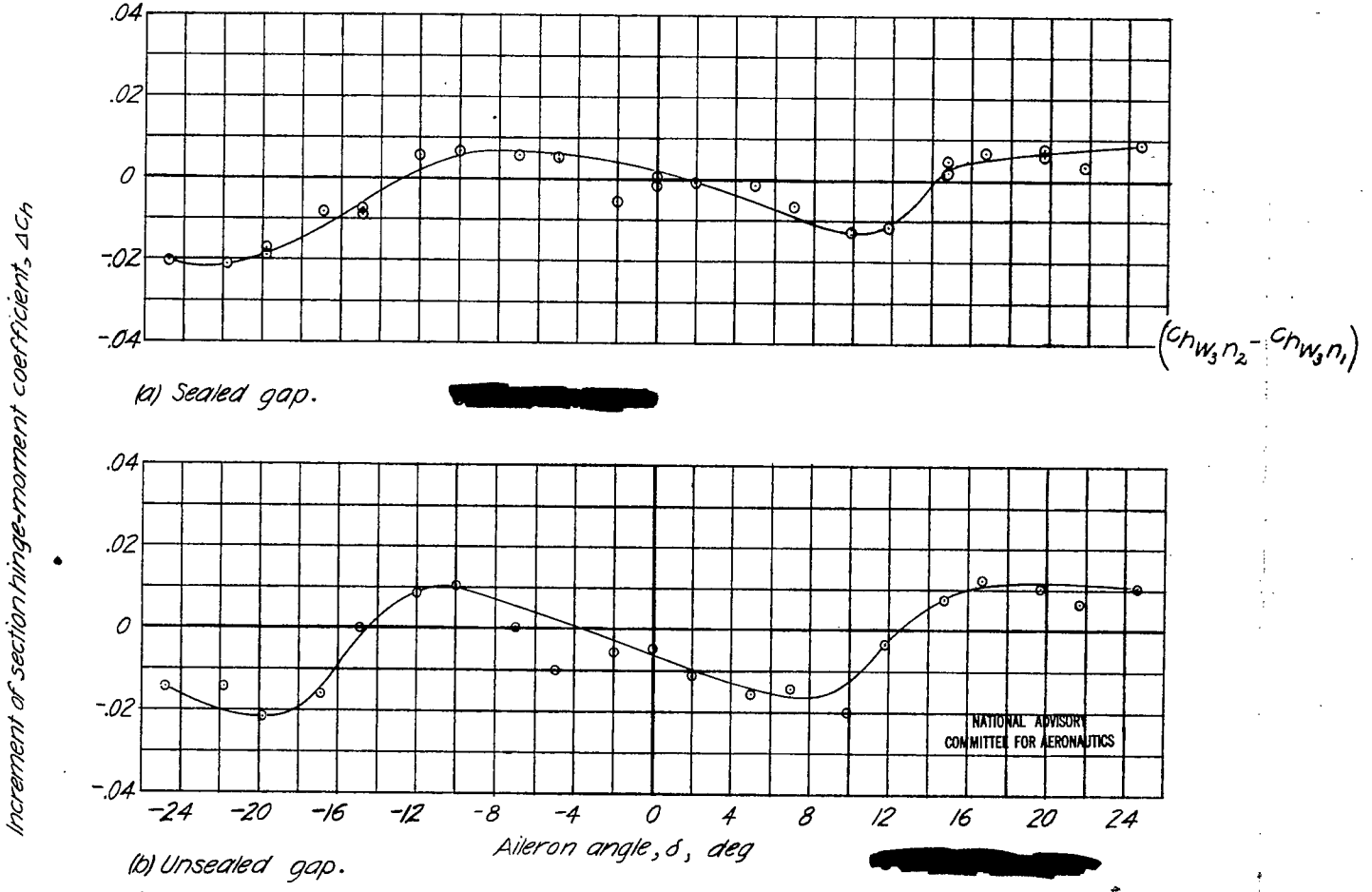

Figure 9.—Effect of rounding aileron nose on section hinge-moment characteristics of aileron. $\alpha_o = 0°$.

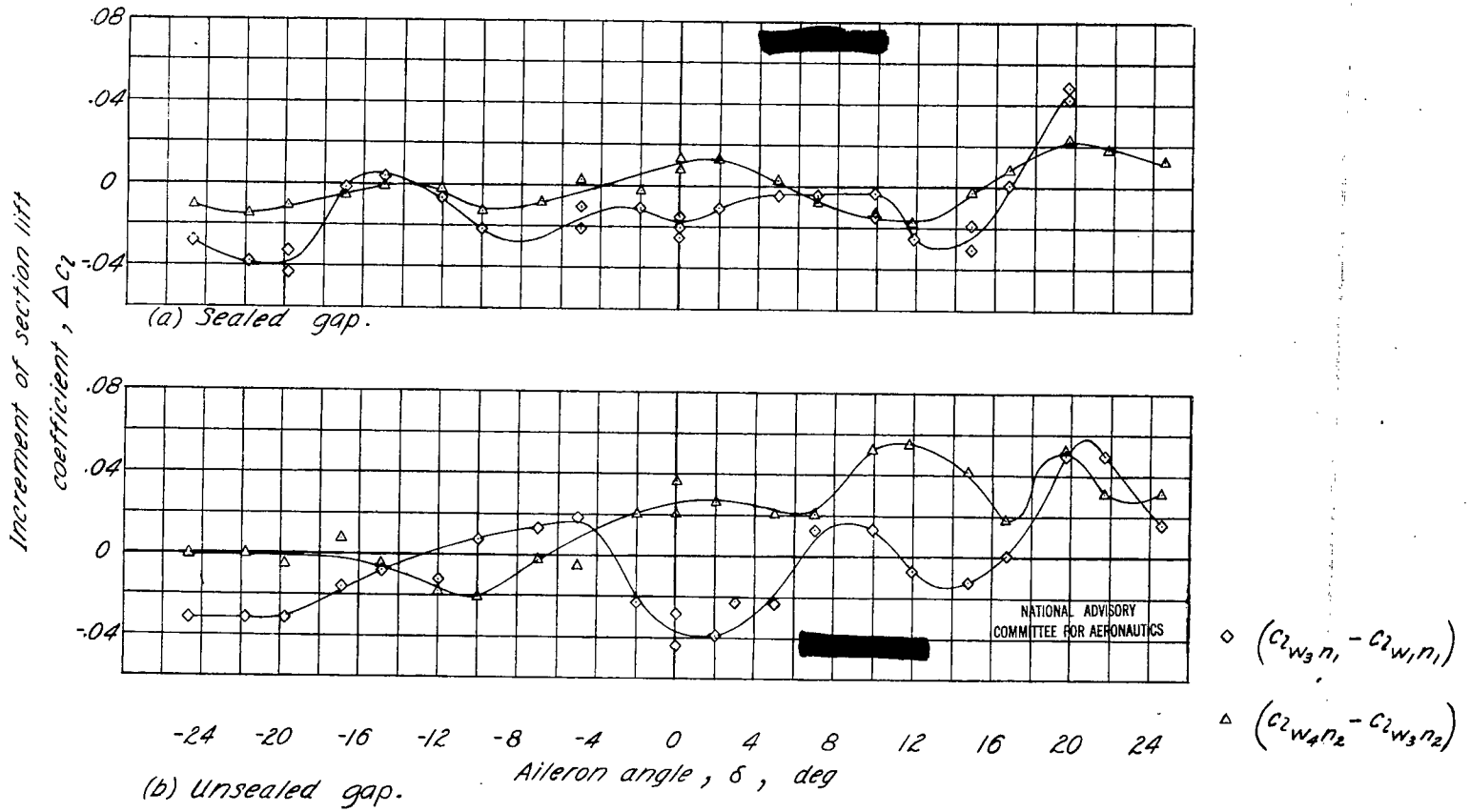

Figure 10. – Effect of rounding airfoil contour adjacent to aileron nose on section lift characteristics of aileron. $\alpha_o = 0°$

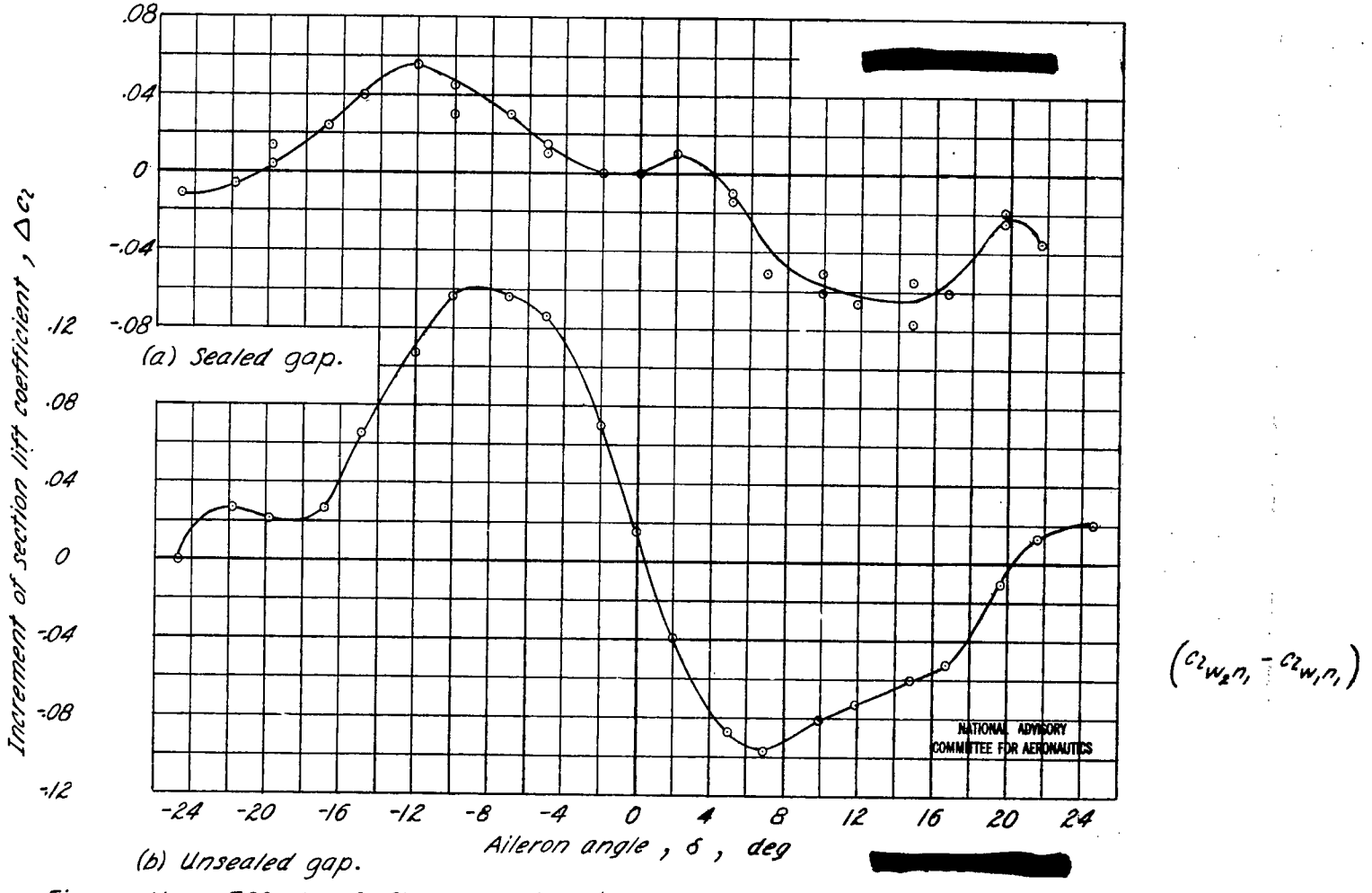

Figure 11 .—Effect of flaring airfoil contour adjacent to aileron nose on section lift characteristics of aileron . $\alpha_0 = 0°$.

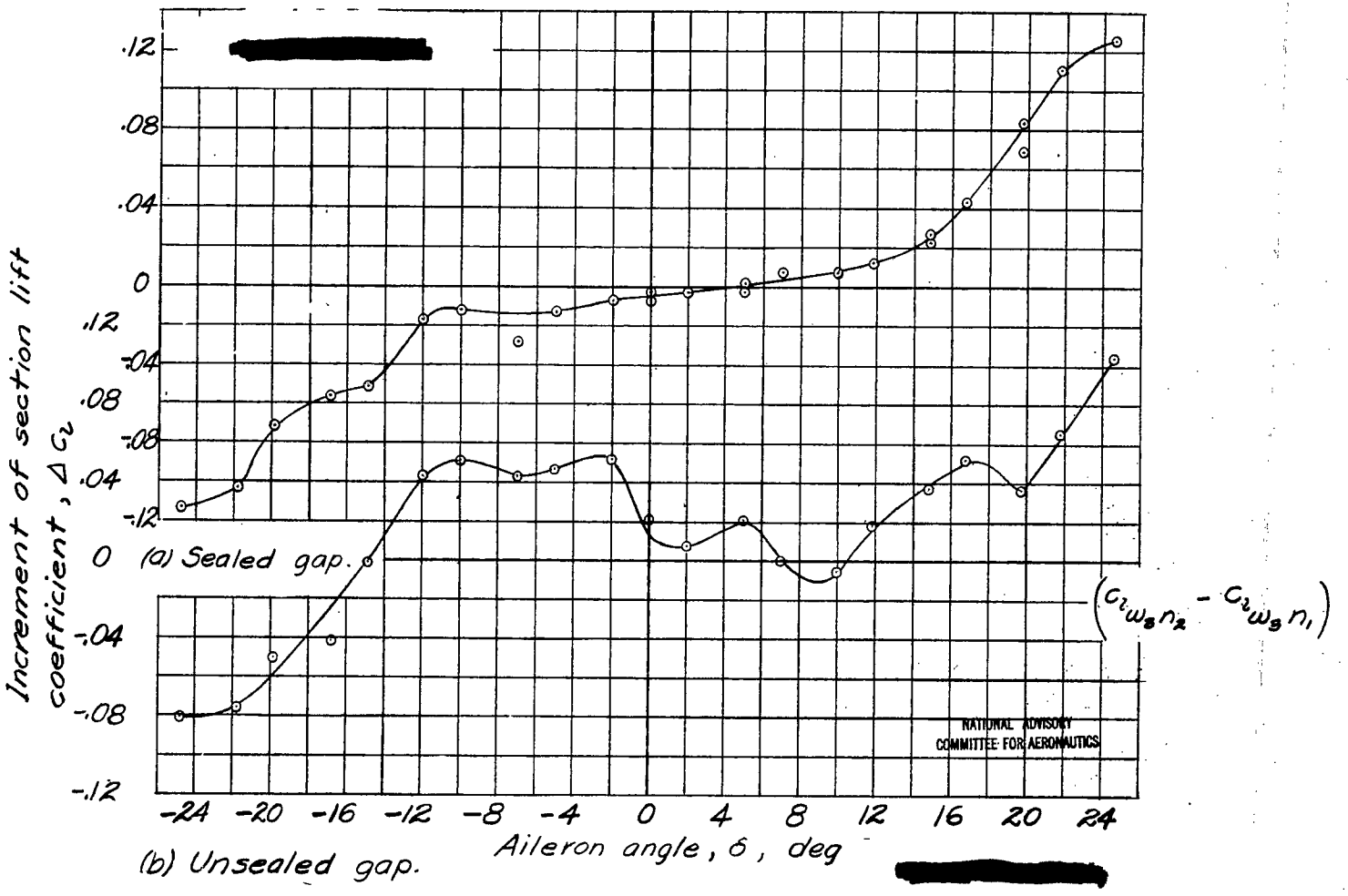

Figure 12.— Effect of rounding aileron nose on section lift characteristics of aileron. $\alpha_o = 0°$.

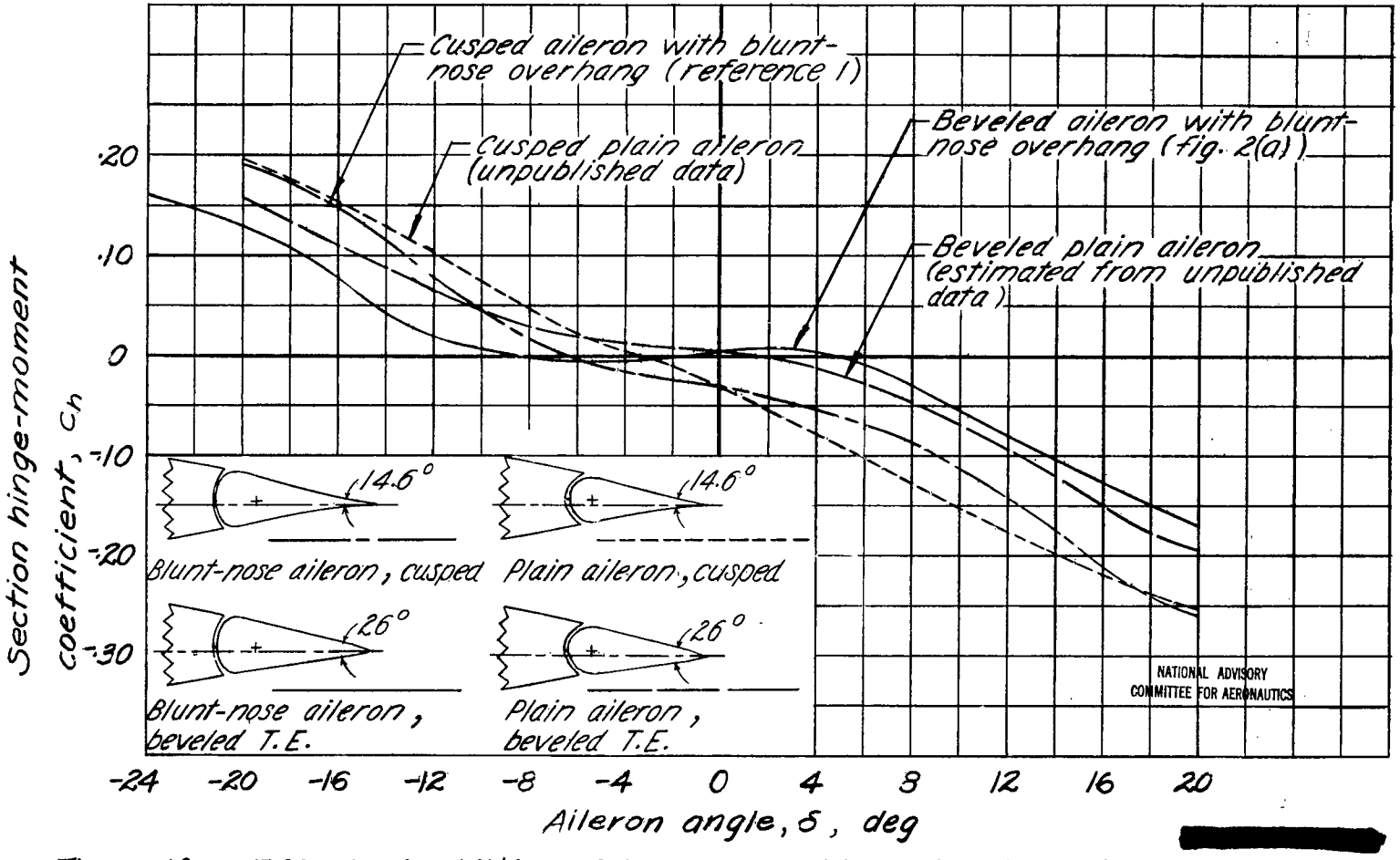

Figure 13.—Effect of addition of beveled trailing edge to plain and blunt-nose ailerons. $\alpha_o = 0°$. All ailerons sealed.

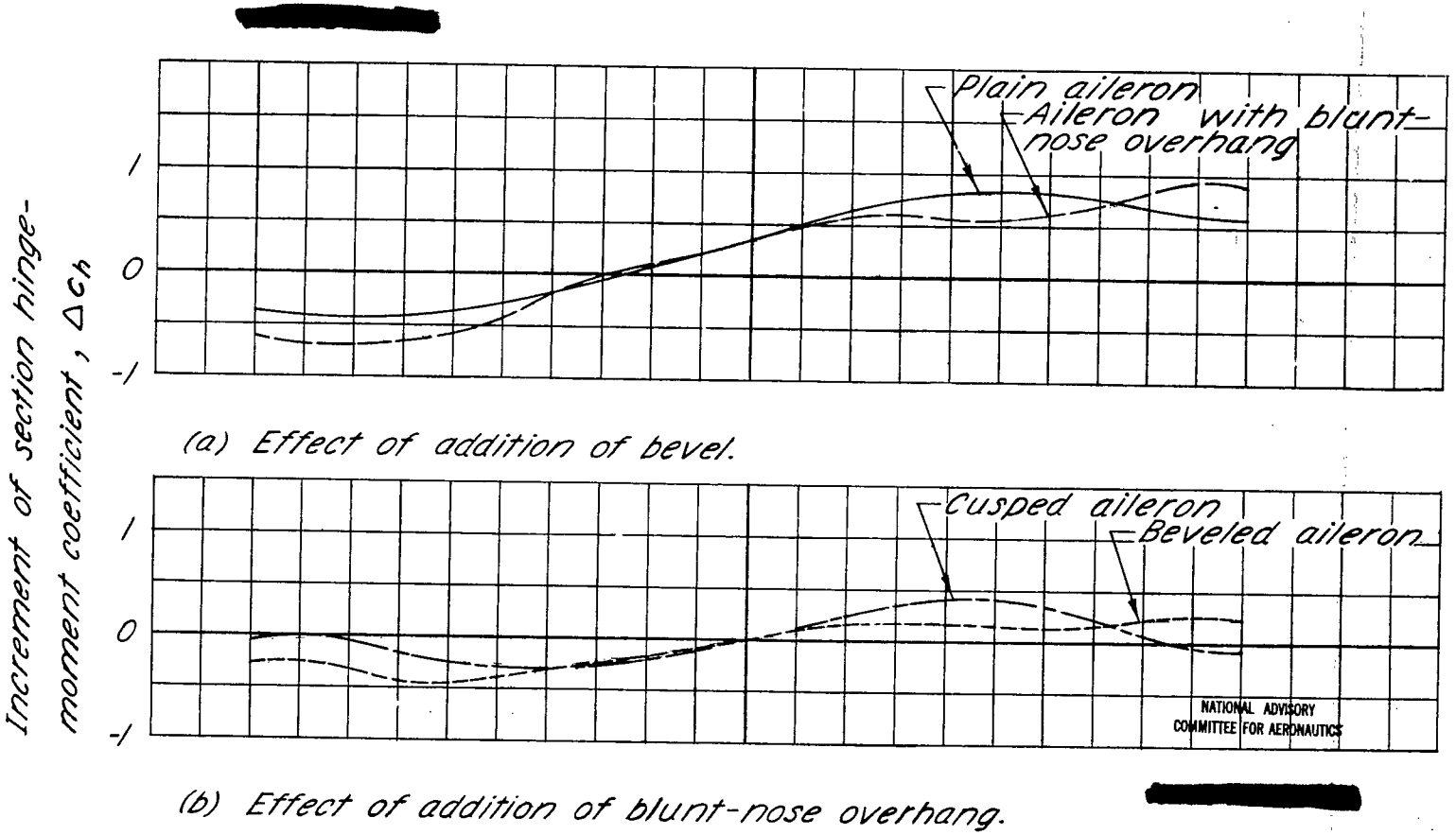

Figure 14.—Increments of section hinge-moment coefficient produced by bevel and overhang. (From fig. 13.)

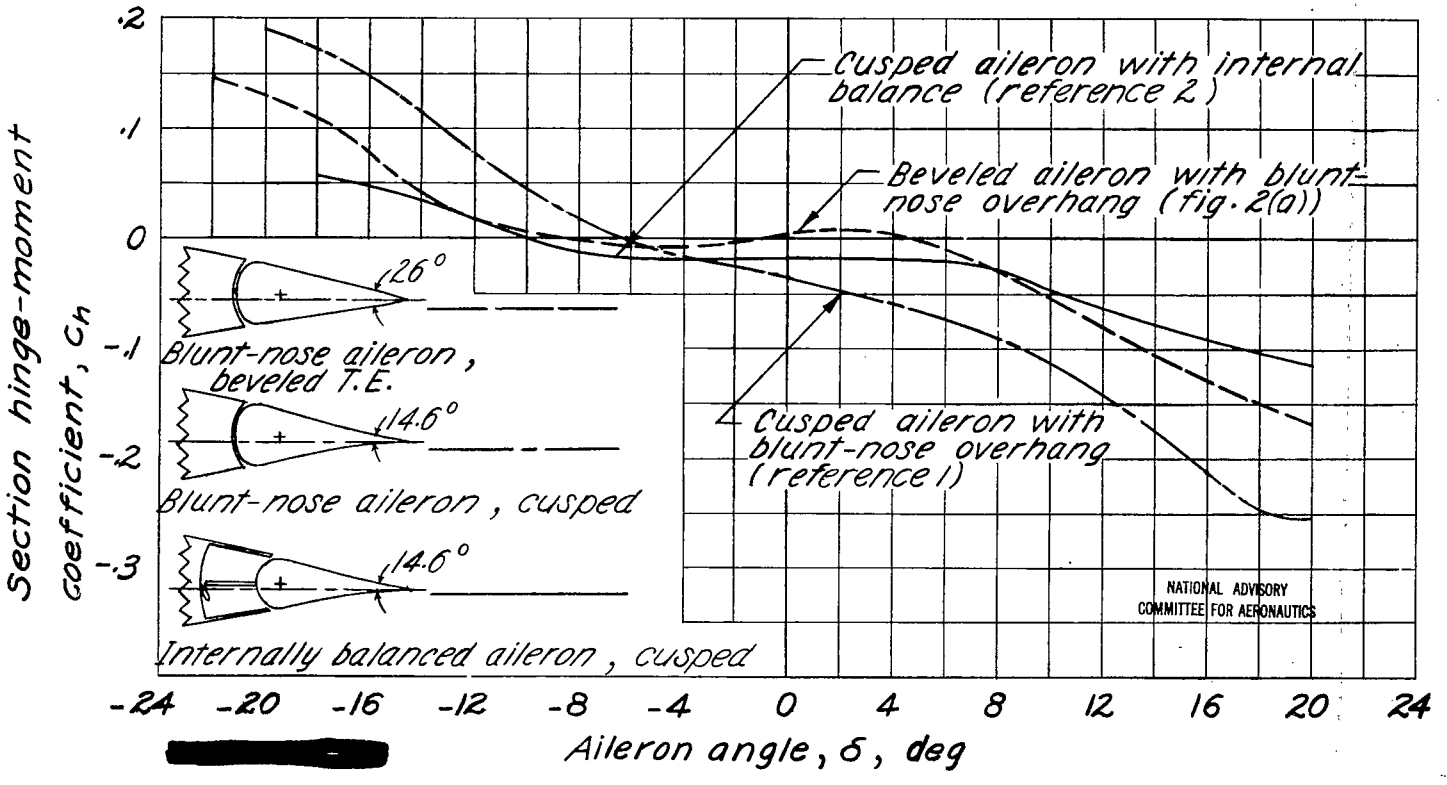

Figure 15.—Variation of section hinge-moment coefficient with aileron angle. $\alpha_o = 0°$. All ailerons sealed.

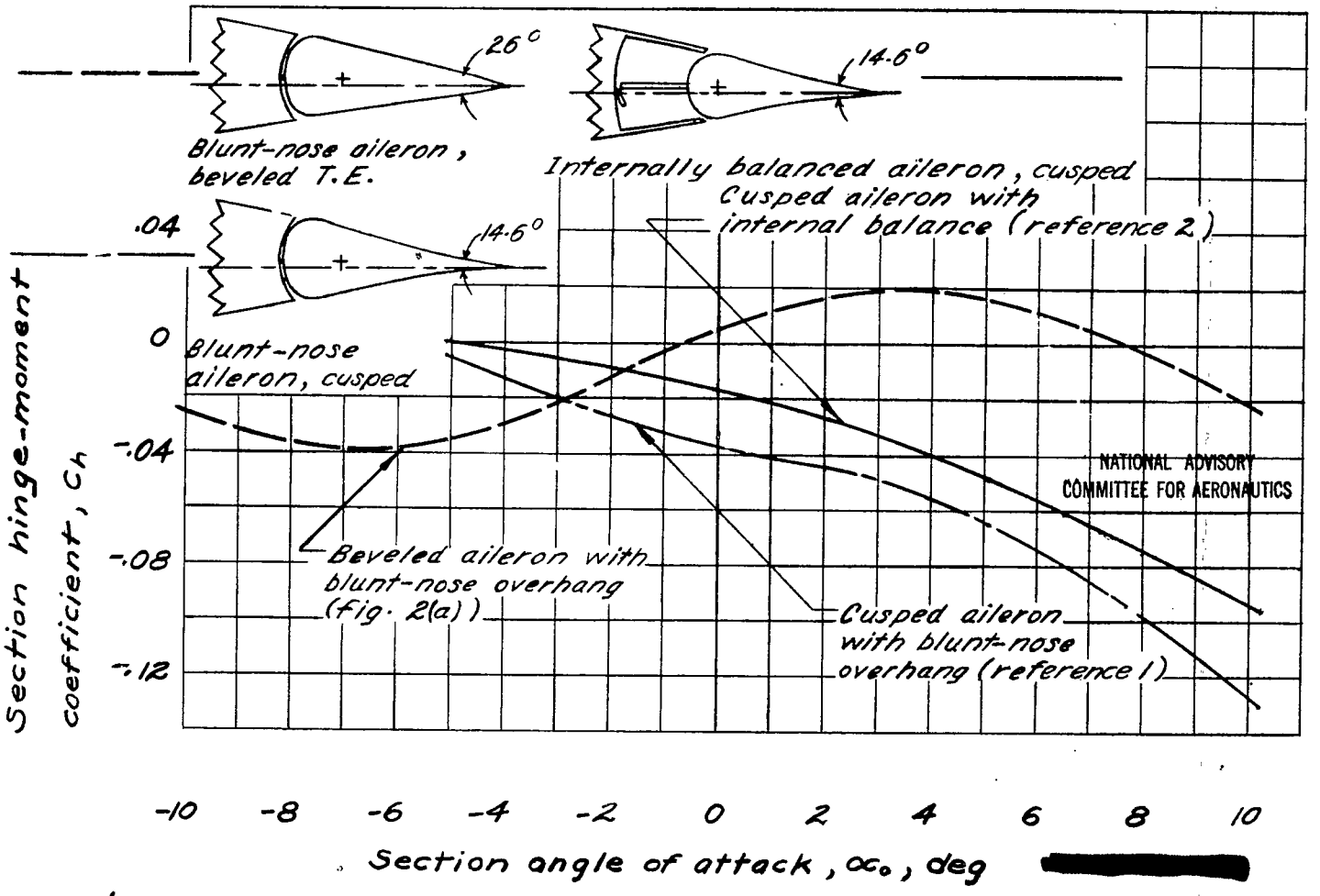

Figure 16.— Variation of section hinge-moment coefficient with section angle of attack. $\delta = 0°$. All ailerons sealed.

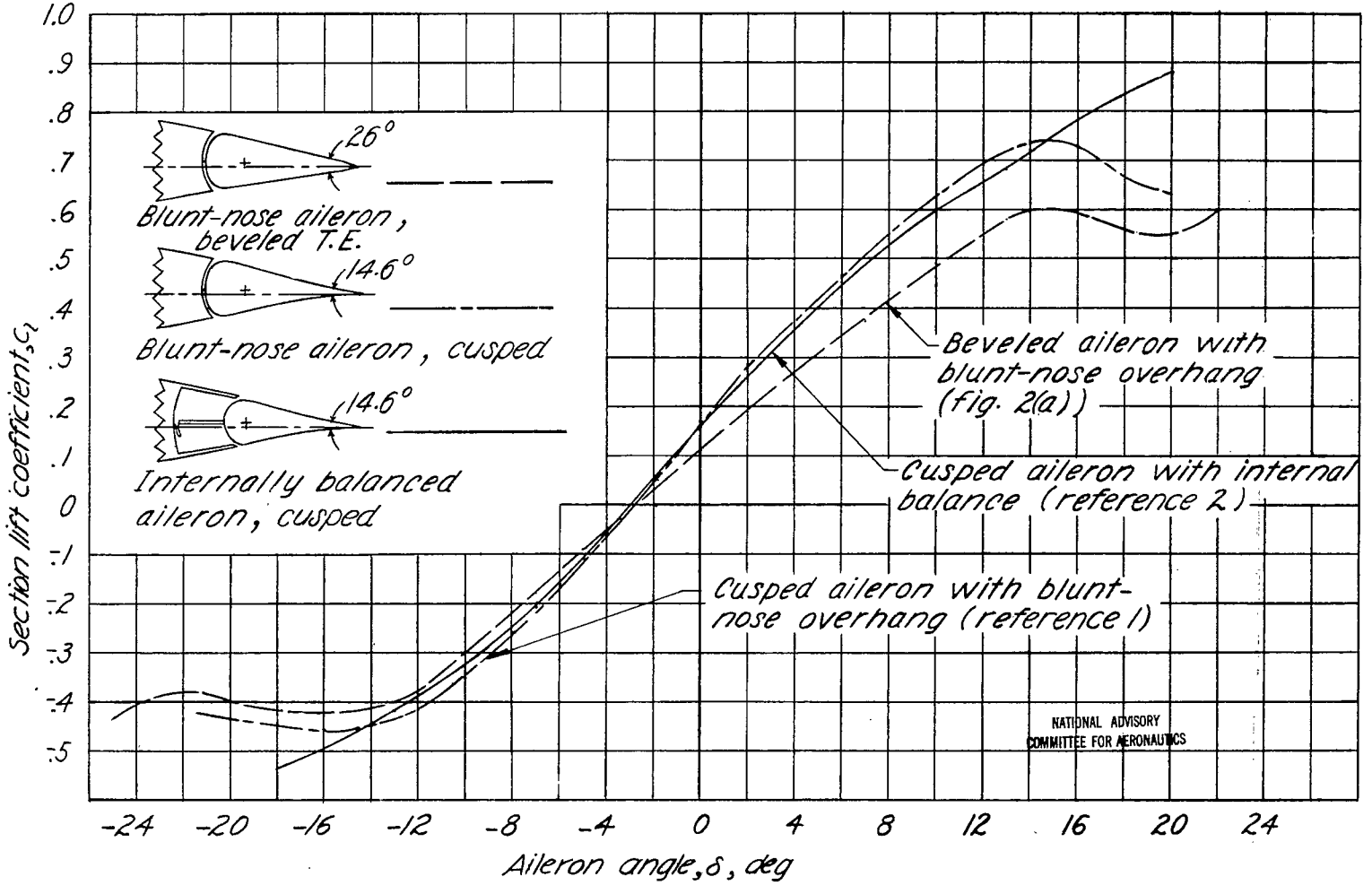

Figure 17 .— Variation of section lift coefficient with aileron angle. $\alpha_o = 0°$. All ailerons sealed.

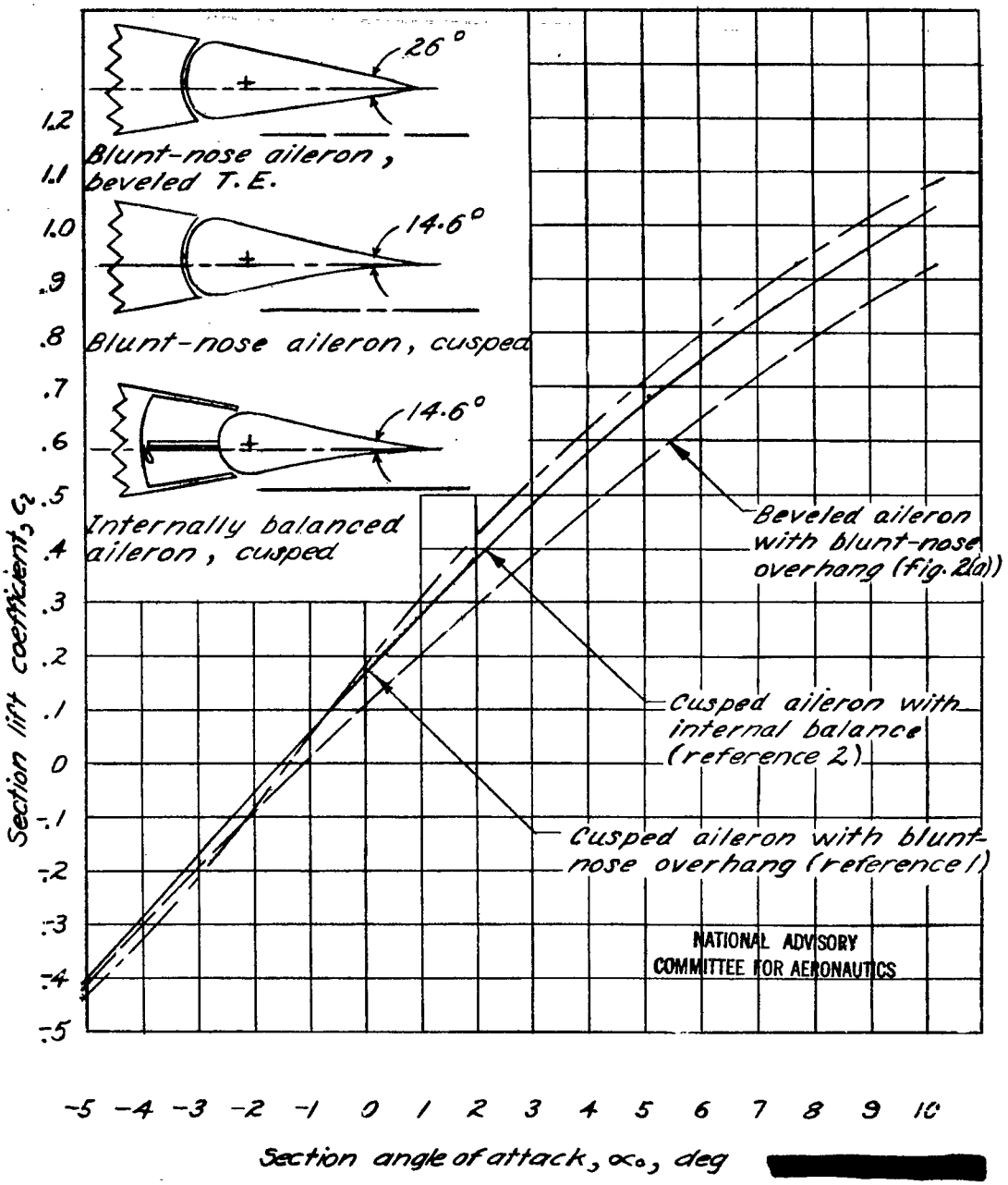

Figure 18. — Variation of section lift coefficient with section angle of attack. $\delta = 0°$. All ailerons sealed.